MK2 degradation as a sensor of signal intensity that controls stress-induced cell fate

Nuria Gutierrez-Prat[a,1,2], Monica Cubillos-Rojas[a,1], Begoña Cánovas[a,1], Antonija Kuzmanic[b], Jalaj Gupta[a,3], Ana Igea[a,4], Elisabet Llonch[a], Matthias Gaestel[c], and Angel R. Nebreda[a,d,5]

[a]Institute for Research in Biomedicine, The Barcelona Institute of Science and Technology, 08028 Barcelona, Spain; [b]Department of Chemistry, University College London, London WC1E 6BT, United Kingdom; [c]Institute of Cell Biochemistry, Hannover Medical School, 30625 Hannover, Germany; and [d]Institució Catalana de Recerca i Estudis Avançats (ICREA), 08010 Barcelona, Spain

Edited by Melanie H. Cobb, University of Texas Southwestern Medical Center, Dallas, TX, and approved April 27, 2021 (received for review November 27, 2020)

Cell survival in response to stress is determined by the coordination of various signaling pathways. The kinase p38α is activated by many stresses, but the intensity and duration of the signal depends on the stimuli. How different p38α-activation dynamics may impact cell life/death decisions is unclear. Here, we show that the p38α-signaling output in response to stress is modulated by the expression levels of the downstream kinase MK2. We demonstrate that p38α forms a complex with MK2 in nonstimulated mammalian cells. Upon pathway activation, p38α phosphorylates MK2, the complex dissociates, and MK2 is degraded. Interestingly, transient p38α activation allows MK2 reexpression, reassembly of the p38α–MK2 complex, and cell survival. In contrast, sustained p38α activation induced by severe stress interferes with p38α–MK2 interaction, resulting in irreversible MK2 loss and cell death. MK2 degradation is mediated by the E3 ubiquitin ligase MDM2, and we identify four lysine residues in MK2 that are directly ubiquitinated by MDM2. Expression of an MK2 mutant that cannot be ubiquitinated by MDM2 enhances the survival of stressed cells. Our results indicate that MK2 reexpression and binding to p38α is critical for cell viability in response to stress and illustrate how particular p38α-activation patterns induced by different signals shape the stress-induced cell fate.

stress | cell survival | p38 | MK2 | MDM2

Cells can respond to stress in a variety of ways through the activation of particular signaling pathways. The initial response is usually aimed at protecting the cell against the insult to facilitate damage recovery and cell survival. However, if the harmful stimulus persists or is not properly resolved, a death program is usually activated that eventually eliminates the damaged cells.

A signaling pathway that is frequently associated with the stress response involves activation of the mitogen-activated protein kinase (MAPK) family member p38α. Upon activation generally achieved by dedicated MAP2Ks, p38α can phosphorylate a variety of substrates in the nucleus and cytoplasm (1, 2). In particular, the activation of p38α is often linked to the activation of MAPK-activated protein kinase 2 (MAPKAPK2 or MK2), and both kinases regulate several stress responses that impinge on cell survival or cell death (3–6). In addition, the p38α–MK2 pathway plays an important role in the regulation of the immune response, and it can also control the proliferation or differentiation of some cell types, which may contribute to physiological responses not necessarily related to stress (7–9). How this pathway can mediate so many different cellular processes is still largely an open question. In many cases, the cellular response mediated by the p38α–MK2 pathway can be determined by the cell type and the stimuli and often engages particular downstream targets. However, other factors, such as signaling dynamics, may also play a role. It has been reported that some MAPKs can perform different functions depending on the amplitude, duration, and frequency of pathway activation (10), but it is still not known whether the p38α-activation dynamics could modulate the cell responses associated with different stimuli.

The formation of protein–protein complexes is important for many biological processes, including signal transduction (11, 12), and changes in their interaction dynamics are crucial for proper sensing of the environmental changes (13). Structural analysis revealed that purified recombinant p38α and MK2 proteins can interact through the p38α docking groove and the MK2 docking motif (14), and further studies addressed the requirements for the formation of the p38α–MK2 complex in vitro (15, 16). Moreover, NMR and X-ray crystallography analysis suggested that p38α-MK2 can form different heterodimers depending on the activation state of p38α (17). However, little is known about how this interaction could be regulated in vivo and whether it modulates the pathway functions.

Given the importance of p38α and MK2 in many cellular processes, the activity of both kinases should be tightly controlled. The down-regulation of p38α activity is known to involve several phosphatases and negative feedback loops (18–22). However, it is not clear how MK2 activity is normally down-regulated.

In this study, we present evidence that the extent of p38α activation regulates MK2 protein levels, which, in turn, have a key role in the pathway output. We show that endogenous p38α and MK2 form a complex in mammalian cells and that, upon p38α activation, the complex dissociates and MK2 is degraded.

Significance

In response to stress, cells can activate several mechanisms that support functionality and survival. However, strong or persistent stresses usually trigger a deleterious answer that leads to cell death. The protein kinases p38α and MK2 are implicated in a stress-signaling pathway. Here, we characterize a molecular mechanism that helps to translate the stress-induced activation of the p38α–MK2 pathway into appropriate biological responses. We show that MK2-expression levels are regulated by the stress intensity and that degradation of MK2 triggered by ubiquitination is linked to cell death. This mechanism will be valuable to better understand the implication of this signaling pathway in pathologies such as inflammatory diseases and cancer.

Author contributions: N.G.-P., M.C.-R., B.C., and A.R.N. designed research; N.G.-P., M.C.-R., B.C., A.K., and E.L. performed research; J.G., A.I., and M.G. contributed new reagents/analytic tools; N.G.-P., M.C.-R., B.C., and A.R.N. analyzed data; and N.G.-P., M.C.-R., B.C., and A.R.N. wrote the paper.

The authors declare no competing interest.

This article is a PNAS Direct Submission.

[1]N.G.-P., M.C.-R., and B.C. contributed equally to this work.

[2]Present address: Molecular Targeted Therapy - Oncology Discovery, F. Hoffmann-La Roche, 4070 Basel, Switzerland.

[3]Present address: Stem Cell Research Center, Sanjay Gandhi Post Graduate Institute of Medical Sciences, 226014 Lucknow, Uttar Pradesh, India.

[4]Present address: Fundación Instituto de Investigación Sanitaria de Santiago de Compostela, 15706 Santiago de Compostela, Spain.

[5]To whom correspondence may be addressed. Email: angel.nebreda@irbbarcelona.org.

This article contains supporting information online at https://www.pnas.org/lookup/suppl/doi:10.1073/pnas.2024562118/-/DCSupplemental.

Published July 16, 2021.

In response to mild stress or to physiological stimuli, the pathway is transiently activated, allowing reformation of the p38α–MK2 complex and concomitant cell survival. However, cells treated with severe stress show sustained p38α activation, which interferes with p38α–MK2 interaction, leading to the irreversible loss of MK2 and cell death. Therefore, our results illustrate an additional mechanism of p38α–MK2 pathway regulation, which might help to predict the cell fate in response to stress.

Results

Stress-Induced p38α Activation Leads to MK2 Down-Regulation. The p38α–MK2 pathway has been connected to several pathologies such as cancer and autoimmune diseases (23–25). Therefore, the pathway activity needs to be strictly controlled for normal physiology. Accordingly, several mechanisms have been reported to account for p38α inhibition (2, 21, 22). In contrast, and despite the well-recognized role of MK2 in the stress response (3, 4, 6), very little is known about how it becomes inactivated. To address this, we monitored the MK2-activation kinetics in cells treated with stress-inducing agents by analyzing two different phosphorylation sites. It should be noted that endogenous MK2 can be expressed as two different protein isoforms (26), explaining why one or two MK2 bands are observed depending on the cell line. We focused on the lower MK2 band (shorter isoform) because it is ubiquitously expressed in cell lines. We found that the ultraviolet-light (UV) and anisomycin-induced phosphorylation of p38α and MK2 unexpectedly correlated with a rapid down-regulation of MK2 protein levels. As a consequence, while p38α was still phosphorylated at later time points, MK2 activity was shut down (Fig. 1 *A* and *B*). This finding was reproduced in several cell lines treated with diverse

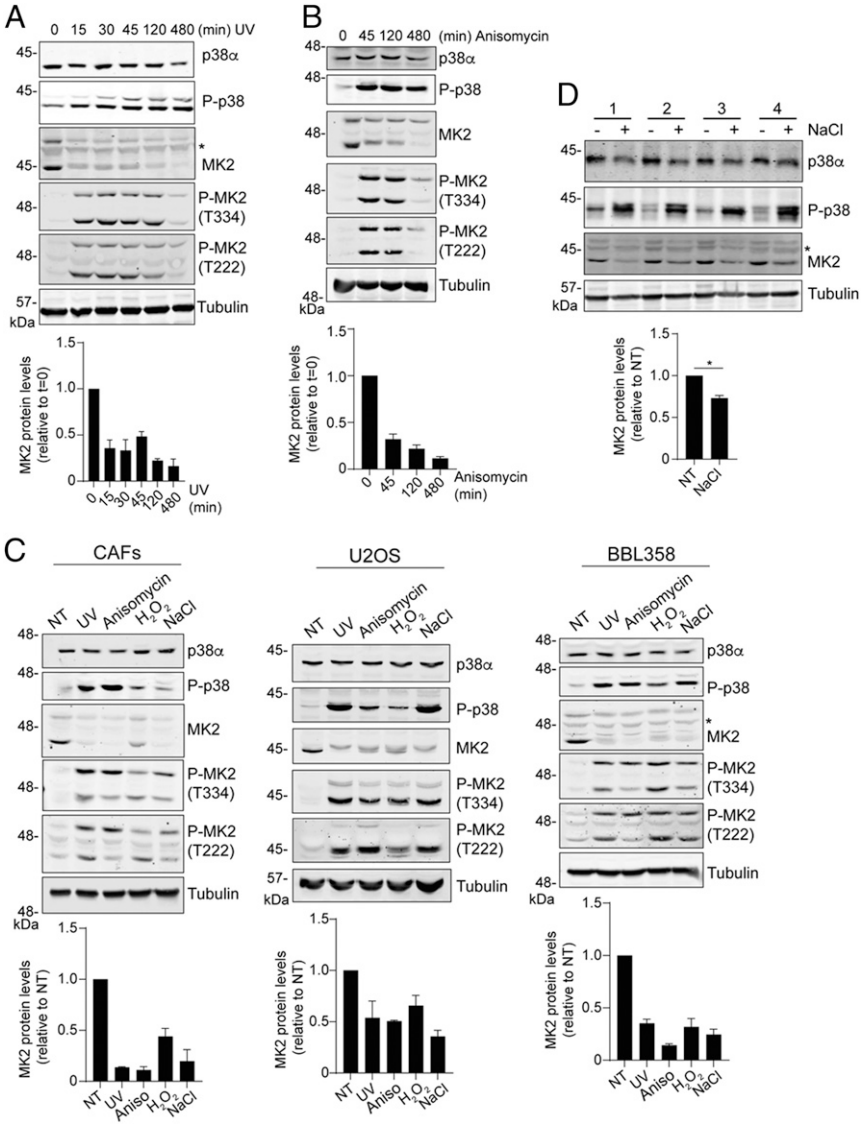

Fig. 1. Sustained p38α activation leads to irreversible MK2 down-regulation. (*A* and *B*) Cancer-associated fibroblasts (CAFs) were stimulated with UV-C (30 J/m^2) (*A*) or anisomycin (20 μM) (*B*) for the indicated times, and cell lysates were analyzed by immunoblotting. The images shown are representative of two independent experiments. The upper band recognized by phospho-p38 antibodies was not consistently detected. (*C*) CAFs, U2OS, and BBL358 cells were treated with UV-C (30 J/m^2), anisomycin (20 μM), H_2O_2 (100 μM), or NaCl (200 mM) for 4 h or were left untreated (NT). Cell lysates were analyzed by immunoblotting. The images shown are representative of two independent experiments. (*D*) Four mammary tumors (1 through 4) were obtained from two different mice expressing MMTV-PyMT and were immediately treated with 300 mM NaCl for 15 min or left untreated (NT), homogenized, and analyzed by immunoblotting. Band intensities were analyzed by ImageJ, and the MK2/Tubulin ratios were represented in the histograms. When two MK2 bands were detected, the lower one (shorter isoform) was considered for quantification. The asterisk indicates a nonspecific band.

stress stimuli (Fig. 1*C*) as well as in mouse mammary tumors treated with osmotic stress (Fig. 1*D*), suggesting that down-regulation of MK2 upon p38α activation is a conserved mechanism for MK2-activity inhibition in the stress response.

MK2 Levels Are Regulated by the Extent of p38α Activation. The stimuli tested in the above experiments are harmful for cells and eventually result in cell death. However, p38α and MK2 are known to be activated also in physiological situations that do not necessarily lead to cell death, such as cytokine production in immune cells or during cell differentiation (7, 27, 28). To analyze the behavior of MK2 in these scenarios, we stimulated bone marrow–derived macrophages (BMDM) with lipopolysaccharide (LPS). We observed that the phosphorylation of p38α and MK2 correlated with the down-regulation of MK2 protein levels at early time points. As LPS induced transient pathway activation, p38α was dephosphorylated at later time points. Strikingly, this correlated with the eventual recovery of MK2 protein levels, which was associated with increased levels of MK2 messenger RNA (mRNA) (Fig. 2 *A* and *B*). A similar pattern was found in cancer-associated fibroblasts (CAFs) incubated with transforming growth factor (TGF)-β, a signal that activates the p38α pathway and influences several processes involved in cell proliferation and differentiation (Fig. 2 *C* and *D*). Altogether, we observed that p38α activation, either in response to stress (anisomycin, UV, or H_2O_2) or to physiological stimuli (LPS and TGF-β), led to MK2 phosphorylation and the concomitant down-regulation of the MK2 protein. However, when the pathway is transiently activated, MK2 levels are eventually restored, which correlates with the cells recovering the homeostatic state. Thus, the different behavior of MK2 following activation suggests a potential link between MK2 dynamics and the cell fate in response to stress.

Different MK2 Levels Induced by p38α Activation Impinge on Cell Viability upon Stress. Our results indicated that the extent of the p38α-pathway activation led to distinct MK2-expression levels and cellular outcomes. Therefore, we hypothesized that MK2 could be more than a mere p38α substrate but rather a modulator of the pathway output. To investigate this possibility, we selected UV irradiation as a stress stimulus that can activate the p38α pathway either in a transient or sustained manner depending on the dose. We found that, in U2OS cells irradiated with 10 J/m^2 (UV10), p38α was transiently activated as observed upon treatment of BMDMs with LPS or CAFs with TGF-β, while the irradiation with 30 J/m^2 (UV30) resulted in a sustained activation of the pathway. In line with our initial observations, the MK2 protein was rapidly down-regulated following p38α activation and restored after treatment with low UV but not with the higher UV dose (Fig. 3*A*), thereby confirming the distinct behavior of the MK2 levels following transient and sustained activation of p38α. The two UV doses used have been linked to distinct cell outcomes (29). We confirmed that, while some UV10 irradiated cells are able to re-enter the cell cycle and proliferate, cells treated with UV30 are mostly committed to die (Fig. 3 *B* and *C*). To analyze the link between the extent of p38α activation and the consequent effects on MK2 protein levels and cell fate, we used a fluorescent reporter (p38α-KTR) (30) (*SI Appendix*, Fig. S1*A*) to simultaneously track both p38α activity and the cellular outcome at the single-cell level. These experiments showed that about half of the cells irradiated with UV10 did not activate p38α at all, explaining the lower MK2 phosphorylation detected in comparison to UV30-treated cells (Fig. 3*D*). Moreover, cells that initially activated p38α in a transient manner did not die during the course of the experiment, while a small fraction of cells that showed a heterogeneous activation pattern died. In contrast, most of the UV30-irradiated cells showed a fast and sustained p38α activation, and they all

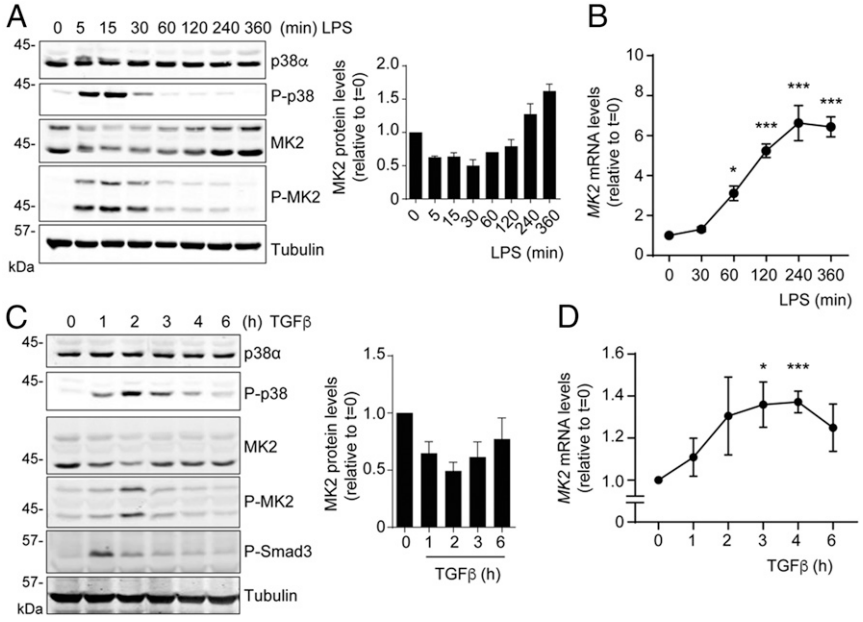

Fig. 2. Transient p38α activation allows MK2 expression recovery. (*A*) BMDMs were starved for 17 h and then stimulated with LPS (10 ng/mL) for the indicated times. Cell lysates were analyzed by immunoblotting. Band intensities were analyzed by ImageJ, and the MK2/Tubulin ratios were represented in the histogram. The images shown are representative of two independent experiments. (*B*) BMDMs were isolated from five different mice and treated as in *A*. RNA was extracted, and the MK2 mRNA levels were determined by qRT-PCR. Data are shown as mean ± SEM. (*C*) CAFs were starved overnight in medium containing 0.5% fetal bovine serum and then treated with TGF-β (5 ng/mL) for the indicated times. Cell lysates were analyzed by immunoblotting. Phospho-Smad 3 antibody was used to confirm TGF-β pathway activation. The histogram represents the MK2/Tubulin ratio determined as in *A*. The images shown are representative of two independent experiments. (*D*) CAFs were treated with TGF-β as in *C*, and MK2 mRNA levels were determined by qRT-PCR. Data are shown as mean ± SEM of five independent experiments. The lower MK2 band (shorter isoform) was considered for quantification. $*P < 0.05$, $***P < 0.001$.

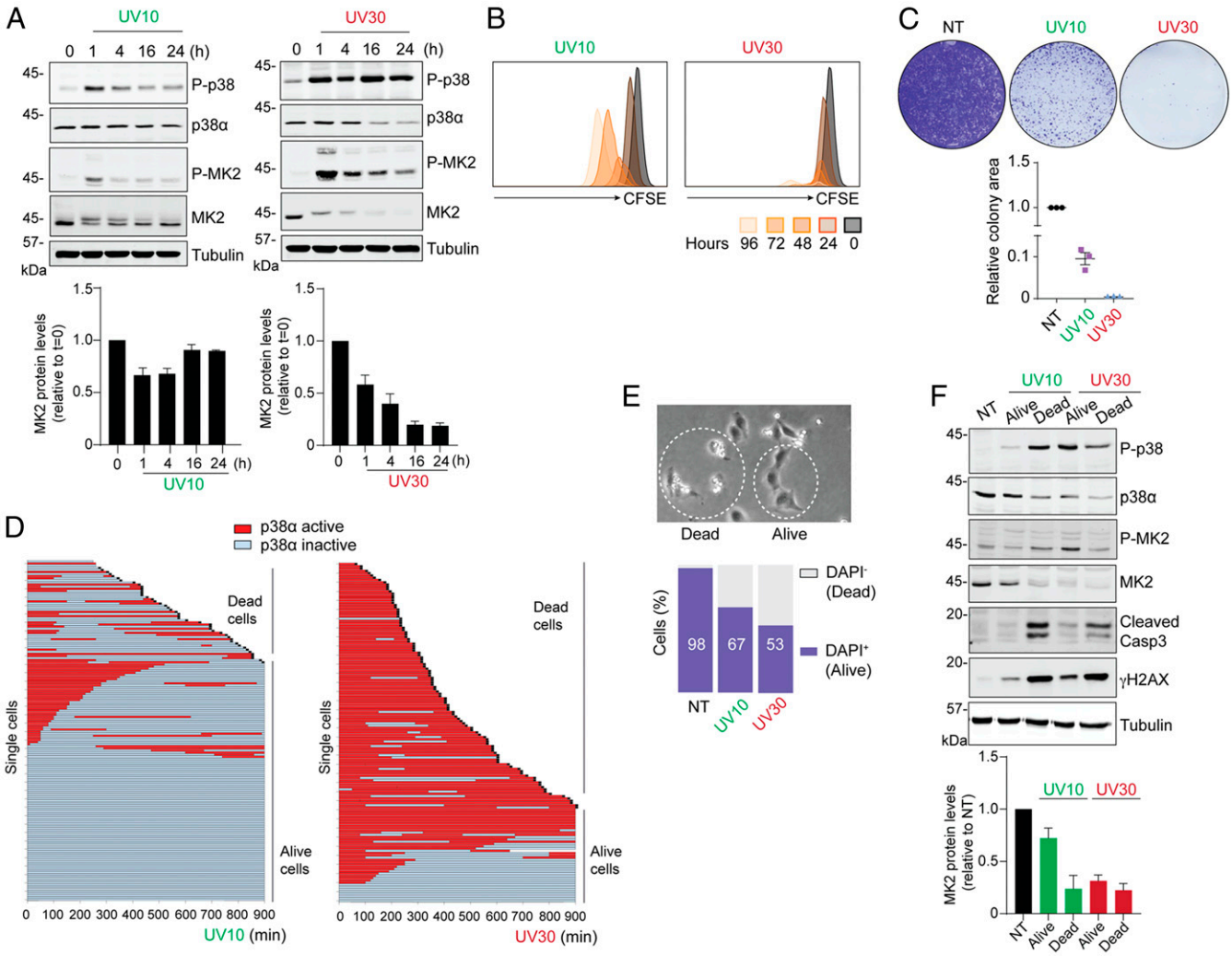

Fig. 3. The extent of p38α activation shapes MK2 levels and cell fate following stress. (*A*) U2OS cells were exposed to UV-C, 10 J/m^2 (UV10), or 30 J/m^2 (UV30) doses and then were incubated for the indicated times. Cell lysates were analyzed by immunoblotting. Band intensities were analyzed by ImageJ, and the MK2/Tubulin ratios were represented in the histograms. The images shown are representative of two independent experiments. (*B*) U2OS cells were stained with the CellTrace CFSE dye and incubated for 24 h. Then, cells were either directly analyzed for CFSE incorporation (0 h) or exposed to UV10 or UV30 as in *A* and analyzed 24, 48, 72, and 96 h later. The intensity of CFSE florescence decreases as peaks move to the left, indicating cell proliferation, and the pick area correlates with the number of cells analyzed. Different times are shown by different colors. The histograms shown are representative data of two independent experiments. (*C*) U2OS cells were exposed to UV10 or UV30 or left untreated (NT) and then were plated to form colonies, which were analyzed 7 d later. The graph shows the colony area relative to NT cells. Data represents mean ± SEM of three independent experiments. (*D*) U2OS cells were infected with lentiviruses expressing a p38α-activity reporter (30) and then were exposed to UV10 or UV30. Single cells were analyzed by time-lapse microscopy for the indicated times. Black ends represent cells that die. The p38α-activity status is shown in red (active) or blue (inactive). (*E*) U2OS cells were treated with UV10 or UV30 and, 24 h later, were collected for 4′,6-diamidino-2-phenylindole (DAPI) staining followed by fluorescence-activated cell sorting (FACS) analysis. The percentages of dead and alive cells are indicated. Representative images of dead (DAPI$^+$) and alive (DAPI$^-$) cells are shown (upper image). (*F*) U2OS cells were treated with UV10 or UV30, and 24 h later, floating and poorly-attached (dead) cells were separated from the well-attached (alive) cells. Lysates from the two cell populations were analyzed by immunoblotting. The histogram represents MK2/Tubulin ratios determined as in *A*. The images shown are representative of three independent experiments.

ended up dying (Fig. 3*D* and *SI Appendix*, Fig. S1*B*). It should be noted that a large proportion of the UV30-irradiated cells that survived more than 15 h either never or just transiently activated p38α, and these are likely the cells that are able to proliferate and form colonies at late time points. Altogether, these results establish a connection between the extent of p38α activation, the MK2 protein levels, and the cellular outcome.

To further support the connection between MK2-expression levels and the restoration of cellular homeostasis following stress, we analyzed the live and dead cell populations after 24 h of UV irradiation (Fig. 3 *E* and *F*). We detected MK2 expression only in the live fraction of UV10-treated cells, corresponding to cells that eventually restore homeostasis and survive. Strikingly, MK2 was not only depleted in all dead cells, independently of the UV dose received, but also in the fraction of UV30-irradiated cells that were alive. This suggests that MK2 is degraded in cells that are subjected to irreversible damage and are meant to die (Fig. 3*F*). Similar results were observed in cells treated with the chemotherapy drug cisplatin, which can activate the p38α pathway to different extents in a concentration-dependent manner (*SI Appendix*, Fig. S1 *C–E*). Altogether, our results support the idea that MK2 protein levels are associated with stress-induced cell fate. Thus, mild stress induces transient activation of the p38α pathway and transient down-regulation of MK2, whose levels are eventually recovered,

allowing the cell to function normally again. However, if the stress persists, p38α activation is sustained, leading to an irreversible MK2 loss that generally results in cell death.

Impaired p38α Binding Results in MK2 Down-Regulation after Pathway Activation. Structural analyses have shown that purified p38α and MK2 proteins can form a complex (14). To further characterize the significance of the p38α–MK2 complex, we initially confirmed that MK2 and p38α coimmunoprecipitated in lysates from cell lines and mouse tissues, indicating that the endogenous proteins are indeed associated in vivo (Fig. 4 *A* and *B*).

Studies using recombinant proteins or based on the fission yeast homologs Sty1 and Srk1 have shown that phosphorylation reduces the binding affinities of the two proteins (31, 32). These observations led us to hypothesize that the phosphorylation of p38α and MK2 upon pathway activation could disrupt the complex, which, in turn, would result in reduced protein stability and the loss of MK2. To address this, we treated cells with UV to activate the pathway and then immunoprecipitated MK2. We confirmed that the MK2 protein remaining in irradiated cells was not able to bind p38α (Fig. 4*C*). These results were confirmed using sucrose gradients, which showed the colocalization of p38α and MK2 in the same fraction from nonstimulated cells. However, in UV-irradiated cells, the colocalization was lost, MK2 levels decreased, and p38α shifted toward lower-molecular-weight fractions, indicating that the complex dissociates and both p38α and MK2 become free (Fig. 4*D*). These results support the idea that p38α-pathway activation results in the separation of the p38α–MK2 complex.

The impact of complex dissociation on MK2 protein stability was further investigated using cycloheximide (CHX) to block protein synthesis. Given that exposure to CHX induces rapid p38α activation (33), and therefore separation of the p38α–MK2 complex, cells were treated with a chemical inhibitor of p38α to avoid MK2 phosphorylation and preserve the complex. We found that, while p38α levels were stable independently of the complex status, the half-life of free MK2 was reduced compared to that of MK2 in complex with p38α (Fig. 4*E*). These observations suggest that p38α-pathway activation results in complex separation and the rapid degradation of MK2, which may constitute a regulatory mechanism to shut down its kinase activity.

To corroborate these results, we analyzed the behavior of MK2 in a p38α knockout (KO) background, in which the complex cannot form. As expected, we observed that MK2 protein levels were decreased in p38α KO cells, and sucrose gradient analysis indicated that the MK2 remaining in these cells appeared in lower-density fractions compared to wild-type (WT) cells (Fig. 4*F*). This confirms that the MK2 protein is less stable when it is not bound to p38α either due to complex dissociation upon pathway activation or due to the absence of p38α. Accordingly, we found a severe down-regulation of MK2 in p38α KO-inducible systems both in vitro and in vivo (*SI Appendix*, Fig. S2 *A* and *B*), which is consistent with studies showing reduced MK2 levels in cells derived from constitutive p38α KO embryos (34). Interestingly, the MK2 mRNA levels were similar in WT and p38α KO cells (*SI Appendix*, Fig. S2*C*), supporting the idea that protein stability modulation plays an important role in the regulation of MK2-expression levels. Moreover, the fact that MK2 is down-regulated in p38α KO cells and tissues indicates a key role for p38α in the regulation of MK2 stability and suggest a minor contribution from other p38 MAPK family members in controlling MK2 levels.

To further characterize the regulation of MK2 degradation, the p38α KO cells were reconstituted with p38α WT or several mutants. Interestingly, all the p38α mutants were able to recover the MK2 levels in p38α KO cells except the mutant with an impaired common docking site (*SI Appendix*, Fig. S3), which is essential for the interactions of p38α with several regulators and substrates including MK2. These results highlight the importance of the interaction with p38α for MK2 stability. Moreover, we extended this study and stimulated, with UV, p38α KO cells reconstituted either with p38α WT or with p38α mutants affecting its kinase domain or the activation-loop phosphorylation (35). We found that cells expressing p38α mutants with impaired kinase activity, which cannot phosphorylate MK2, were unable to down-regulate MK2 expression as efficiently as the cells expressing p38α WT (Fig. 4*G*), suggesting that MK2 phosphorylation is required for its down-regulation.

Taken together, our results indicate that p38α and MK2 form a complex in homeostasis and that stress-induced activation of both kinases results in complex disruption. If stress persists, the phosphorylated MK2 is unable to reassemble the complex and is degraded.

MK2 Released from p38α Has Reduced Stability and Is Degraded by the Proteasome. In eukaryotic cells, protein degradation is usually regulated by two processes: autophagy and the ubiquitin–proteasome system (36). To address how the free MK2 protein unbound to p38α is degraded, we used inhibitors of both processes. We found that inhibition of the proteasome, but not of autophagy, prevented MK2 degradation following pathway activation (Fig. 5*A*). Notably, given the sustained activation of the p38α pathway upon UV irradiation, the MK2 protein that accumulates with proteasome inhibitors was phosphorylated and failed to interact with p38α (Fig. 5*B*), further supporting the idea that phosphorylation impairs the binding of the two proteins and that free MK2 is rapidly degraded by the proteasome. In addition, blocking proteasome function also partially prevented the MK2 down-regulation observed in p38α KO cells (Fig. 5*C*) as well as in another UV-treated cell line (Fig. 5*D*), suggesting that this mechanism of MK2-activity regulation is probably conserved.

The proteasome is a multisubunit complex that exists in cells in two main forms, the 20S proteasome, which is the catalytic core particle, and the 26S proteasome that incorporates a 19S regulatory subunit to both ends of the 20S form. The 19S subunit contains ATPases and deubiquitinating enzymes and is involved in the recognition of the polyubiquitin chains of the substrate and its translocation to the catalytic core (37). Although most proteins rely on ubiquitination for proteasomal degradation, it has been proposed that some proteins can be degraded by the 20S proteasome in a ubiquitin-independent manner (38, 39). To dissect the proteasome-mediated degradation of MK2, we incubated UV-treated cells with inhibitors of the 20S (MG132 [MG] and Bortezomib [BTZ]) or 19S proteasome subunits (b-AP15 [AP] and O-phenanthroline [OPA]) (40, 41). As a positive control for protein degradation mediated by the 26S proteasome, we analyzed the p53 levels. We found that all the proteasome inhibitors tested induced MK2 protein accumulation in a similar way to p53 (Fig. 5 *E* and *F*), indicating that MK2 is degraded by the 26S proteasome complex in a ubiquitin-dependent manner.

MDM2 Ubiquitin Ligase Controls MK2 Degradation. Protein ubiquitination is mainly regulated by the interaction between specific E3 ubiquitin ligases and their target substrates (42). E3 ligases catalyze the ubiquitin transfer reaction and control the binding between the E2 ubiquitin–conjugating enzyme and the substrate (43). Using a bioinformatics platform that predicts E3 ligase–substrate interactions (44), we identified MK2 as a potential substrate for SMURF1, STUB1, and MDM2 (*SI Appendix*, Fig. S4*A*). To validate their potential implication, we down-regulated each of these E3 ligases (*SI Appendix*, Fig. S4*B*) and then irradiated the cells with UV to induce p38α-pathway activation and MK2 degradation. We found that only cells deficient for MDM2, but not the other two E3 ligases, showed enhanced MK2 protein levels after UV irradiation (Fig. 6*A*). Accordingly, knockdown of this E3 ligase partially recovered the levels of MK2 in p38α KO

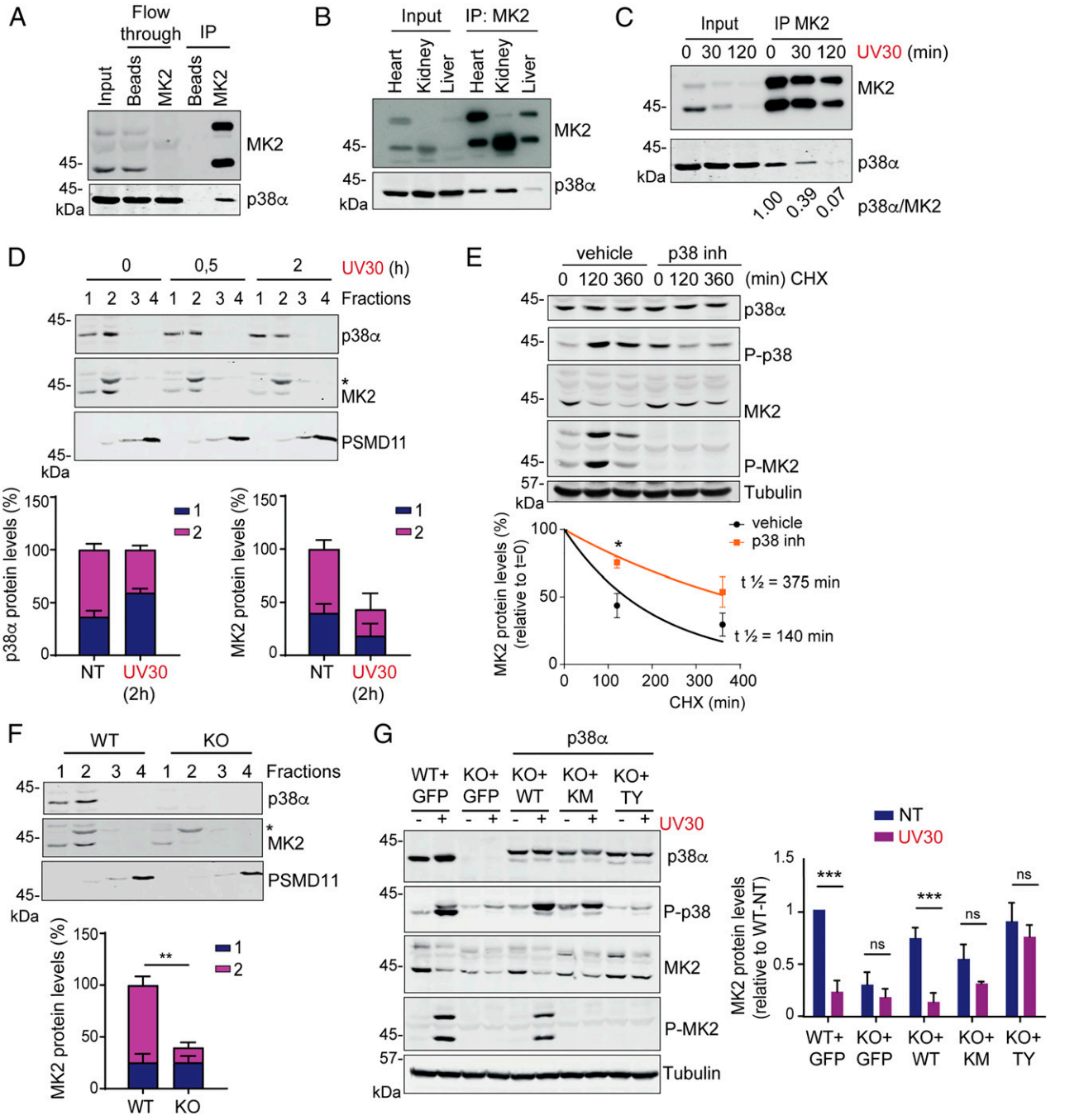

Fig. 4. MK2 levels are regulated by its interaction with p38α. (*A* and *B*) Lysates from CAFs (*A*) and the indicated mouse tissues (*B*) were immunoprecipitated with MK2-Trap_A (MK2) or agarose beads (Beads) and then were analyzed by immunoblotting. (*C*) CAFs were treated with UV-C 30 J/m^2 (UV30), and the cell lysates were immunoprecipitated with MK2-Trap_A (IP MK2) and then analyzed by immunoblotting. Band intensities were analyzed by ImageJ, and the p38α/MK2 ratios are indicated. (*D*) CAFs were treated with UV30 for the indicated times, and lysates were separated on 20 to 28% sucrose gradients. Collected fractions were analyzed by immunoblotting. PSMD11 was used as a marker for high-molecular-weight complexes. Band intensities were analyzed by ImageJ. The histograms show the p38α and MK2 levels in fractions 1 and 2, which are normalized to the total p38α and MK2 amounts in untreated cells (NT). Data represents mean ± SEM of two independent experiments. (*E*) CAFs were pretreated with the p38 inhibitor BIRB796 (p38 inh, 10 μM), to preserve the p38α–MK2 complex, or the vehicle dimethyl sulfoxide (DMSO) for 2 h and then incubated with CHX (50 μg/mL), which induces p38α activation and complex separation. At the indicated times, lysates were analyzed by immunoblotting. The estimated MK2 half-lives are indicated (t 1/2). Data represents mean ± SEM of three independent experiments. (*F*) Lysates from WT and p38α KO CAFs were separated on 20 to 28% sucrose gradients. Collected fractions were analyzed by immunoblotting. The asterisk in the blot indicates a nonspecific band. The 26S proteasome component PSMD11 was used as a marker for high-molecular-weight complexes. Band intensities were analyzed by ImageJ software. The histogram shows the quantifications of the MK2 levels in fractions 1 and 2, which are normalized to the total MK2 amount in WT cells. Data represents mean ± SEM of three independent experiments. Significant differences refer to fraction 2. (*G*) WT and p38α KO CAFs expressing Myc-p38α WT or the mutants K53M (KM) and Thr180A/Y182F (TY), or a GFP-expressing vector as control, were either left untreated or treated with UV30 for 1 h. Cell lysates were analyzed by immunoblotting. Band intensities were analyzed by ImageJ, and the MK2/Tubulin ratios are represented in the histogram. Data represents mean ± SEM of three independent experiments. When two MK2 bands were detected, the lower one (shorter isoform) was considered for quantification. $^{**}P < 0.01$, $^{***}P < 0.001$.

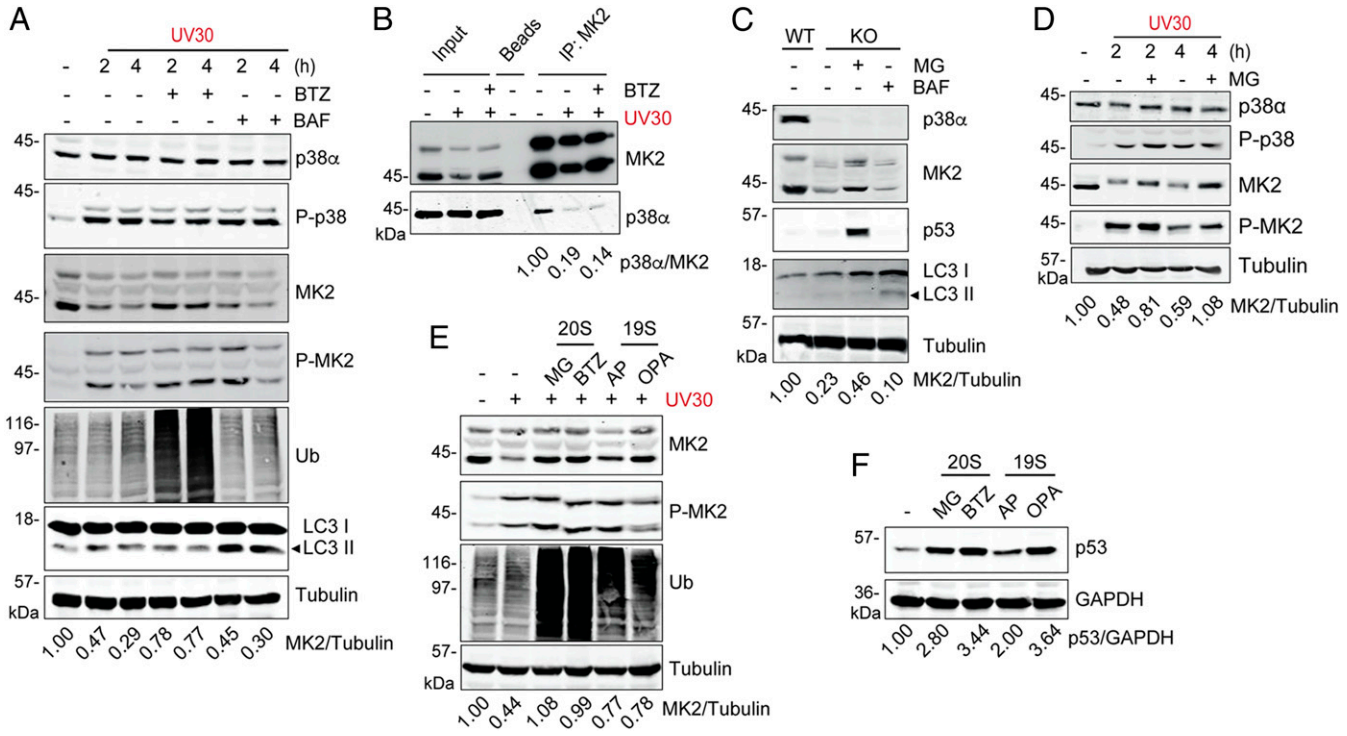

Fig. 5. MK2 is degraded by the proteasome upon dissociation from p38α. (*A*) WT CAFs were treated with the proteasome inhibitor BTZ (100 nM) or the autophagy inhibitor Bafilomycin A1 (BAF, 400 nM), stimulated with UV-C 30 J/m^2 (UV30), and then incubated for the indicated times. Lysates were analyzed by immunoblotting. Ubiquitinated (Ub) and LC3II proteins were used as markers for proteasome or autophagy inhibition, respectively. The arrowhead indicates LC3II accumulation. The upper band recognized by phospho-p38 antibodies was not consistently detected. (*B*) CAFs were pretreated with BTZ for 2 h, irradiated with UV30, and then incubated for 4 h. Cell lysates were immunoprecipitated with MK2-Trap_A (MK2) or agarose beads (Beads) and analyzed by immunoblotting. (*C*) WT and p38α KO CAFs were treated with the proteasome inhibitor MG (20 μM) or with BAF for 16 h, and lysates were analyzed by immunoblotting. p53 and LC3II proteins were used as markers for proteasome and autophagy inhibition, respectively. (*D*) U2OS cells were pretreated with MG and then stimulated with UV30 for 2 and 4 h. Cell lysates were analyzed by immunoblotting. (*E*) CAFs were preincubated with the proteasome inhibitors MG, BTZ, AP (3 μM) or OPA (200 μM) for 2 h, irradiated with UV30, and then incubated for 4 h. Cell lysates were analyzed by immunoblotting. Ubiquitinated (Ub) proteins were used as a control for proteasome inhibition. (*F*) CAFs were preincubated with the proteasome inhibitors MG, BTZ, AP, or OPA for 6 h. Cell lysates were analyzed by immunoblotting with p53 antibodies to confirm proteasome inhibition. In all cases, the images shown are representative from two independent experiments, band intensities were analyzed by ImageJ, and the lower MK2 band (shorter isoform) was considered for quantification.

cells (Fig. 6*B*), pointing to MDM2 as a potential regulator of the degradation of MK2 when separated from p38α.

Next, we used purified recombinant proteins to confirm that MK2 was a direct substrate of MDM2. We found that MK2 was ubiquitinated by MDM2 in vitro to a similar extent to p53, a well-known MDM2 substrate (45, 46) (Fig. 6*C* and *SI Appendix*, Fig. S4*C*). Moreover, using mass spectrometry analysis, we found that K188, K371, K374, and K385 were ubiquitinated upon incubation with MDM2 (Fig. 6*D* and *SI Appendix*, Fig. S5). Interestingly, structural analysis indicated that these four lysines are buried inside the p38α–MK2 complex. Specifically, K188 is buried within the dimerization interface, while K371, K374, and K385 are located in the MK2 docking motif that also interacts with p38α (Fig. 6*E*). Therefore, these sites will be difficult to ubiquitinate when MK2 is bound to p38α, explaining why MK2 can only be targeted (and degraded) by MDM2 once it is released from p38α. To confirm that MDM2 can ubiquitinate these residues, we generated an MK2 mutant with the four lysines mutated to arginines (MK2 4K/R) and found that MK2 ubiquitination was significantly impaired in the 4K/R mutant compared to the WT protein (Fig. 6*F*), indicating that the identified lysines are involved in MK2 ubiquitination by MDM2.

Irreversible Degradation of MK2 Facilitates Cell Death upon Severe Stress. Our results demonstrate that MK2 regulation is mainly dictated by protein stability, which, in turn, depends on its interaction with p38α to form a stable complex that avoids its ubiquitination by MDM2. Moreover, we have shown that sustained p38α activation and the consequent irreversible loss of MK2 correlates with cell death. Therefore, we hypothesized that MK2 activity has a protective role in stress and that its degradation-mediated inactivation would impair cell survival. To test this idea, we used the MK2 4K/R mutant that exhibits a defective ubiquitination pattern and is predicted to show increased protein stability upon dissociation from p38α. MK2 KO mouse embryonic fibroblasts (MEFs) were reconstituted with MK2 WT or the 4K/R mutant and then were irradiated with a high UV dose to induce sustained p38α-pathway activation, which results in complex dissociation and cell death. We observed that the levels of the MK2 4K/R mutant were not substantially reduced following UV irradiation, at least during the time analyzed, confirming that this mutant was more stable than its WT counterpart (Fig. 7*A*). Interestingly, cells expressing this more stable 4K/R form showed reduced UV-induced cell death compared to cells expressing MK2 WT (Fig. 7*B*). These results support the hypothesis that stabilization of MK2, and therefore a higher and/or more sustained MK2 activity, results in enhanced cell viability in response to stress.

To confirm this idea, cells were stimulated with high doses of UV in the presence of p38α or MK2 inhibitors. In agreement with MK2 having a pro-survival role, blocking the activity of either p38α or MK2 increased UV-induced cell death (Fig. 7*C*). Of note, p38α inhibition avoids MK2 phosphorylation, and therefore MK2 protein levels were increased in these cells (Fig. 7*D*). However, the MK2 that accumulates is not phosphorylated, lacks kinase activity,

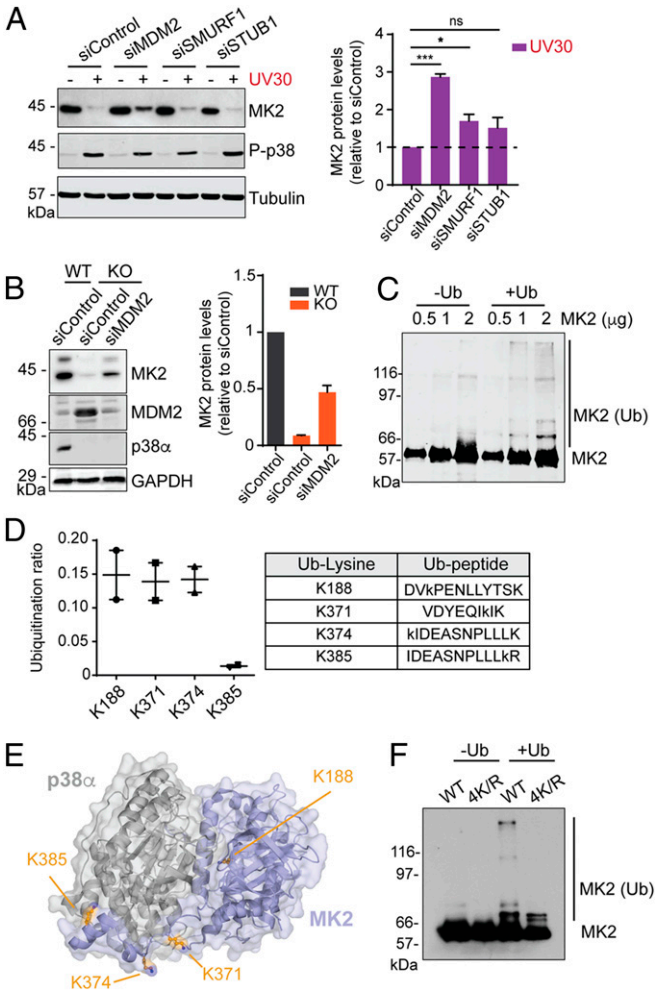

Fig. 6. MDM2 ubiquitinates MK2. (*A*) U2OS cells were transfected with siRNAs against MDM2, SMURF1, and STUB1, or a nontargeting control, stimulated with UV-C, 30 J/m^2 (UV30) and then incubated for 4 h. Cell lysates were analyzed by immunoblotting. Band intensities were analyzed by ImageJ, and the MK2/Tubulin ratios in UV30-treated cells were represented in the histogram. Data represents mean ± SEM of three independent experiments. (*B*) WT and p38α KO CAFs were transfected with siRNA control or against MDM2 and were analyzed by immunoblotting. The histogram represents the MK2/Tubulin ratios determined as in *A*. Data represents mean ± SEM of two independent experiments. (*C*) The indicated amounts of GST-MK2 protein were incubated with ubiquitin, E1, E2 (UBE2D3), and GST-MDM2 for 1 h at 37 °C. Samples incubated without ubiquitin were used as negative controls. Ubiquitinated MK2 [MK2(Ub)] was detected by immunoblotting with an MK2 antibody. The images shown are representative from two independent experiments. (*D*) MK2 residues ubiquitinated by MDM2 and the corresponding peptides as identified by mass spectrometry. The ubiquitination ratio was calculated as the number of peptide spectrum matches with the indicated residue ubiquitinated versus nonubiquitinated. (*E*) MK2-ubiquitinated lysines are highlighted in orange in the context of the p38α–MK2 complex (Protein Data Bank ID: 2OZA). The image was produced using PyMOL version 2.0. (*F*) Purified GST-MK2 and GST-MK2 4K/R proteins (2 μg) were incubated with ubiquitin, E1, E2 (UBE2D3), and GST-MDM2 for 1 h at 37 °C. Samples incubated without ubiquitin were used as negative controls. Ubiquitinated MK2 [MK2(Ub)] was detected by immunoblotting with a MK2 antibody. The images shown are representative from two independent experiments.

and therefore cannot exert its pro-survival function, explaining the increased cell death observed despite MK2 protein accumulation. Altogether, our results indicate that MK2 signaling regulates the viability of stressed cells. Since sustained stress is deleterious for cells, it is conceivable that MK2 degradation serves as a regulatory mechanism to limit this pro-survival function, eventually leading to cell death of the irreversibly damaged cells.

Discussion

Consistent with the evidence implicating p38α and MK2 in the regulation of many cellular stress responses, aberrant activation of this pathway has been connected to several human diseases such as inflammatory disorders and cancer (24, 25, 47). It is therefore important for cellular and organismal homeostasis that the activity of the p38α–MK2 pathway is strictly controlled. It is known that p38α can be inactivated by several types of phosphatases, whose expression sometimes can be induced by p38α signaling itself (21, 22), and negative feedback loops can further modulate the pathway activity (18, 20). In contrast, very little is known about how MK2 activity is physiologically shut off. Notably, MK2 amplification correlates with poor prognoses in some tumors, and high MK2 levels in multiple myeloma are required for tumor growth and drug resistance (48, 49). Hence, dysregulated MK2 expression can alter cell homeostasis leading to disease, supporting the importance of elucidating the mechanisms that control MK2 activity to understand the implication of the p38α–MK2 pathway in pathogenesis.

Our results show a key role for proteolysis in controlling the extent of MK2 activity. In homeostasis, endogenous MK2 and p38α form a complex. When the pathway is activated, p38α phosphorylates MK2, leading to complex dissociation, and the two kinases become available to phosphorylate their respective downstream targets. We demonstrate that, upon separation from p38α, MK2 can be ubiquitinated, which triggers its degradation by the proteasome. A decreased number of phosphorylated (active) MK2 molecules in the cell ensures that the signal is turned off. Interestingly, the inactivation of p38α and MK2 seems to be based on different mechanisms, offering the opportunity to specifically target MK2-regulated functions such as cytokine production or RNA metabolism without affecting functions regulated by other p38α substrates. Our study has focused on MK2, one of the best-characterized effectors of p38α, but a similar mechanism could operate for other substrates that can associate with p38α in a stable manner, as might be the case for MK3, which contains a similar docking motif to MK2 (50). However, other proteins that interact with p38α seem to be regulated in completely different ways, as shown for MKK6 (18) and ATF2 (51), despite also having a docking motif. It should be noted that the ability of endogenous MK2 to form a stable complex with p38α in nonstimulated cells has not been reported for other substrates.

We identify the E3 ubiquitin ligase MDM2 as an important regulator of MK2 protein stability. We found that MDM2 can ubiquitinate MK2 on four lysine residues that are predicted to be buried inside the interface between MK2 and p38α, which is consistent with the fact that MK2 is only degraded when separated from p38α. MDM2 is a critical regulator of the p53 protein in response to various stress signals (52, 53). Given that the p53 and p38α–MK2 pathways have a key role in safeguarding cellular homeostasis, MDM2 stands as a common regulator to engage an integrated cellular response to stress. Accordingly, it is tempting to propose that MDM2 could function as a hub that coordinates the pro-survival role of MK2 signaling with the apoptotic programs driven by p53.

Our work indicates that the dynamic interaction between p38α and MK2 is regulated by the kinetics of p38α activation (transient versus sustained) and makes an important contribution to the pathway output (*SI Appendix*, Fig. S6). Thus, MK2 levels are recovered when the pathway is transiently activated, such as in response to cytokine stimulation (54). In this scenario, the MK2 mRNA accumulates, probably due to transcriptional activation, allowing the reexpression of the MK2 protein when p38α is no longer active. Newly synthesized MK2 then binds to dephosphorylated p38α, forming a heterodimer again and restoring cell homeostasis.

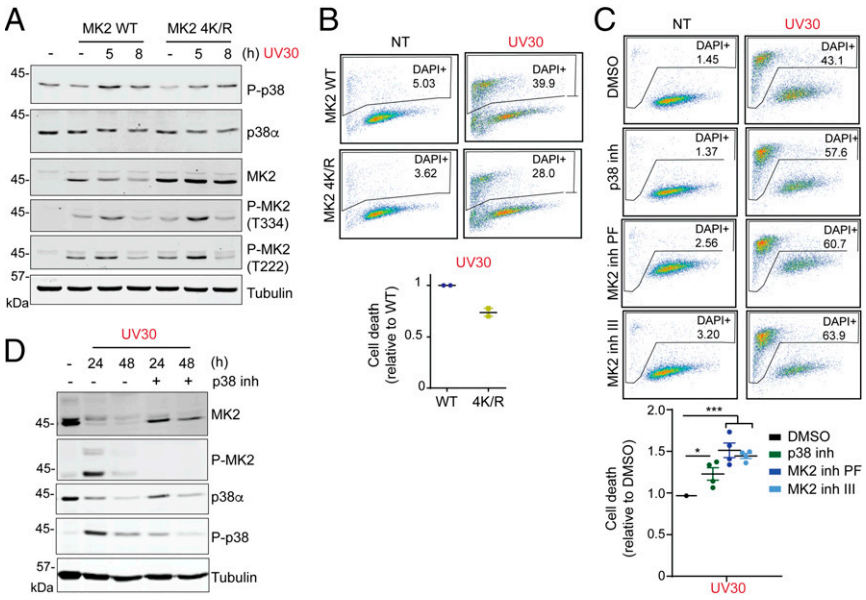

Fig. 7. MK2 activity modulates cell survival in response to stress. (*A*) MK2 KO MEFs were electroporated with either MK2 WT or the mutant 4K/R (K188R, K371R, K374R, and K385R), stimulated with UV-C, 30 J/m^2 (UV30), and then incubated for 5 and 8 h. Cell lysates were analyzed by immunoblotting. (*B*) MEFs expressing MK2 WT or MK2 4K/R were stimulated with UV30 and then were incubated for 16 h. Cell death was analyzed by DAPI staining and normalized to the value observed in UV30-treated MK2 WT cells at 16 h. Data represents mean ± SEM of two independent experiments. (*C*) U2OS cells were pretreated with the p38α inhibitor PH797804 (p38 inh, 2 μM) and the MK2 inhibitors PF3644022 (PF, 2.5 μM) and MK2 inhibitor III (10 μM) or vehicle (DMSO) for 4 h and then were exposed to UV30. After 24 h, cells were harvested and stained with DAPI to analyze cell death by FACS. Data were normalized to the cell death observed in UV30-treated DMSO cells. Data represents mean ± SEM of four independent experiments. (*D*) U2OS cells were pretreated with PH797804 (p38 inh) or DMSO (-) for 2 h, treated with UV30, and then incubated for the indicated times. Cell lysates were analyzed by immunoblotting.

However, under conditions of persistent or severe stress (55, 56), p38α activation is sustained and MK2 cannot bind to the phosphorylated p38α, leading to irreversible MK2 down-regulation and cell death. Importantly, it has been recently reported that mice expressing a constitutively active p38α mutant show reduced MK2-expression levels in several tissues, which correlates with a significant body-weight loss, suggesting that the mechanism of MK2 down-regulation that we propose may also operate in vivo (57). Notably, in response to sustained stress, MDM2 has been reported to show a decreased affinity for phosphorylated p53 (58), suggesting that it could shut down the MK2 pro-survival role without affecting the p53-regulated proapoptotic program.

The ability to facilitate the survival of cells subjected to stress is a conserved function of the p38α pathway. In response to genotoxic stress such as UV, MK2 has been reported to activate the G_2/M cell cycle checkpoint via Cdc25B/C phosphorylation (3) and can also phosphorylate the RNA-binding proteins NELFE and RBM7, enabling an RNA polymerase II transcriptional response that is crucial for the survival of stressed cells (4, 59). Furthermore, phosphorylation of the tumor necrosis factor receptor–interacting kinase RIPK1 by MK2 suppresses the pro-apoptotic and pro-necroptotic functions of this key molecule upon inflammatory and stress stimuli (27). These mechanisms could potentially explain the pro-survival role of the p38α–MK2 pathway that we observe following severe stress. However, in some cell types, p38α signaling has been reported to contribute to UV-induced apoptosis, which has been related to p53 (60, 61) or to changes in proapoptotic molecules and survival signals (62). Therefore, it is conceivable that the cell type, the duration of the stimulus, and the interplay with other signaling pathways may all contribute to define the final outcome of p38α activation in stressed cells. In line with this idea, there is evidence that in vivo roles of MK2 are highly dependent on the context. For example, a lack of MK2 can protect mouse skin from UV-B–induced keratinocyte death (6) but enhances DNA damage and chemotherapy cytotoxicity in KRAS-induced lung tumors (63). In fact, the function of MK2 has been reported to depend on the genetic background and, in particular, p53 status (64).

It is important to note that p38α is not the only signaling pathway that controls DNA damage–induced cell death. For example, cell-to-cell variability in JNK activity has been proposed to contribute to the timing and probability of death in UV-exposed cells (65). Our results suggest that the MK2 protein expression levels, as determined by the extent of p38α activation, may provide an additional source of variability that affects the biological outcome. However, considering that MK2 in several cell types can potentially contribute to resolving tissue damage (66), it is difficult to predict the consequences of interfering with MK2 activity in vivo.

In summary, we describe an additional layer of regulation of the p38α-signaling pathway, which is based on the balance between MK2 protein degradation and de novo synthesis and controls its ability to modulate the cellular response to stress. This mechanism relies on the ability of p38α to bind to and stabilize MK2, which is required to recover cell homeostasis. The inability to reassemble the p38–MK2 complex in response to strong or sustained stress may function as a sensor of irreversible damage leading to cell death.

Methods

Cell Treatments. To deplete p38α, *Mapk14*$^{lox/lox}$ UBC-Cre-ERT2 CAFs were treated with 100 nM 4-hydroxytamoxifen (Sigma-Aldrich, no. H7904-5MG) for 48 h. For the inhibition of p38α, we used 2 μM PH797804 (Selleckchem, S2726), 10 μM SB203580 (Axon MedChem, 1363), or 10 μM BIRB796 (Axon MedChem, 1358). MK2 was inhibited using 2.5 μM PF3644022 (Sigma-Aldrich, PZ0188) or 10 μM MK2 III (Calbiochem). The activation of the p38α pathway was induced by exposure to either 10 J/m^2 or 30 J/m^2 UV using a UVC-500 crosslinker (Amersham Biosciences), 200 mM NaCl, 100 μM hydrogen peroxide (Sigma-Aldrich, H1009), 20 μM anisomycin (Sigma-Aldrich, A9789), 10 ng/mL LPS (Sigma-Aldrich, L4005), or 5 ng/mL TGF-β1 (Prepotech, 100-21). The proteasome was inhibited with 20 μM MG (Sigma-Aldrich, no. C2211), 100 nM Bortezamib (Selleckchem, PS-341), 3 μM b-AP15 (Selleckchem, S4920),

or 200 μM O-phenanthroline (MERK Millipore, 516705). To inhibit autophagy, we used 400 nM Bafilomycin A1 (Sigma-Aldrich, B1793).

MK2 Immunoprecipitation. To immunoprecipitate endogenous MK2, we used single-domain antibodies against MK2 bound to agarose beads (MK2-trap_A, Chromotek, mta-20). As a control, we used the same agarose beads (Chromotek, nbab-20). Cells or tissue samples were lysed and processed as recommended in the manufacturer's protocol. Briefly, cell lysates were extracted with the buffer provided, and the protein content was quantified using the RC DC Protein Assay Kit I (Bio-Rad, 5000111). A total of 25 μL MK2-Trap_A or control agarose beads were incubated overnight with 500 μg cell lysate rotating at 4 °C. The next day, beads were recovered, washed three times, resuspended in 1× sodium dodecyl sulphate-polyacrylamide gel electrophoresis (SDS-PAGE) sample buffer and heated for 5 min at 95 °C. Immunoprecipitated proteins were analyzed by immunoblotting.

Sucrose Gradients. CAFs were trypsinized, harvested, and resuspended in 25 mM Hepes, 0.1 mM EDTA, 12.5 mM $MgCl_2$, 10% Glycerol, 0.1 M KCl, 0.1% Nonidet P-40, 1 mM dithiothreitol (DTT), and 1× EDTA-free complete protease inhibitor mixture (Roche, no. 1187358000). Lysates were incubated for 15 min on ice and centrifuged 15 min at 16,000 × *g*. The supernatant (1 mg) was loaded on top of a 4-mL linear sucrose gradient (20 to 28%) in the same buffer. Gradients were centrifuged at 156,500 × *g* in a Beckman Coulter MLS-50 rotor for 16 h at 4 °C. Fractions of 930 μL were collected from top to bottom and were analyzed by immunoblotting.

Determination of the MK2 Protein Half-Life. CAFs were treated or not treated with a p38α inhibitor and exposed to CHX (50 μM, Sigma-Aldrich, C6255). Cells were collected at different times and subjected to immunoblotting with an MK2 antibody, using Tubulin as a loading control. The intensity of the bands was determined using ImageJ software. The half-life was determined by fitting the data to an exponential decay equation using the GraphPad Prism computer program (Graphpad Software, Inc.).

Down-Regulation of E3 Ubiquitin Ligases by siRNAs. U2OS cells or p38α KO CAFs were transfected with small interfering RNAs (siRNAs) using Lipofectamine RNAi MAX transfection reagent (Thermo Fisher, 13778150) following the manufacturer's protocol. After transfection, cells were incubated 24 h in antibiotic-free media, split, and analyzed 48 h later. The following siRNAs were purchased from Ambion Life Technologies: SMURF1 5′CCAGCACUAUGAUCUAUAUTT 3′ (no. 120615); STUB1 5′GAGCUAUGAUGAGGCCAUCTT 3′ (no. 215047); MDM2 5′GCCAUUGCUUUUGAAGUUATT 3′ (no. 122296).

In Vitro Ubiquitin Conjugation Reaction. Ubiquitination reactions were performed by using an MDM2/p53 Ubiquitination kit following the manufacturer's protocol (Boston Biochem, K-200B). Briefly, recombinants E1, E2, and GST-MDM2 were incubated with either His-p53, GST-MK2, or GST-MK2 4K/R for 60 min at 37 °C. The reaction was terminated by adding 1× SDS-PAGE sample buffer and heating at 95 °C for 5 min. Samples were analyzed in a 10% polyacrylamide gel that was run for 5 h, followed by immunoblotting with antibodies against p53 or MK2. GST-MK2 and GST-MK2 4K/R were expressed in *Escherichia coli* and purified following standard protocols.

CellTrace Carboxyfluorescein Succinimidyl Ester–Based Proliferation Assays. Carboxyfluorescein succinimidyl ester (CFSE) was used to measure cell proliferation. Each time that a cell divided, CFSE was transferred equally among the daughter cells, reducing fluorescence in half. Typically, up to 10^6 cells/mL were labeled with 1 μL CFSE (Thermo Fisher, C34554) and incubated for 24 h. The next day, control cells were collected and analyzed by flow cytometry while the rest of the cells were treated with either low UV or high UV doses and incubated for 24, 48, 72, and 96 h. After the incubation time, cells were analyzed by flow cytometry using exactly the same protocol as for control cells.

Cell Viability Assays. U2OS cells were trypsinized, and 3×10^5 cells were plated in triplicate in 6-well plates. Cells were incubated for 24 h and then were irradiated with the indicated doses of UV and allowed to grow for 7 d. Then cells were fixed in 4% paraformaldehyde (Aname, 15710) and stained with crystal violet (Sigma-Aldrich, HT90132). The colony area was measured using ImageJ.

Statistical Analysis. Data are expressed as average ± SEM. The statistical analysis was performed by using Student's *t* test for the comparison of two groups or ANOVA for multiple groups, using GraphPad Prism Software 6.01 (GraphPad Software, Inc.). *P* values are expressed as $*P \leq 0.05$, $**P \leq 0.01$, and $***P \leq 0.001$.

Data Availability. All study data are included in the article and/or *SI Appendix*.

ACKNOWLEDGMENTS. We thank Bernat Crosas (Instituto de Biología Molecular de Barcelona) for insightful suggestions on ubiquitination assays, Sergi Regot (Johns Hopkins University School of Medicine) for the p38α-KTR reporter, Jessica Vitos-Faleato and Nevenka Radic for critical reading of the manuscript and helpful discussions, Raquel Batlle for the generation of mesenchymal stem cells, and all members of the A.R.N. laboratory for support and discussions. We are grateful to Marina Gay, Marta Vilaseca, and members of the Institute for Research in Biomedicine (IRB Barcelona) Mass Spectrometry and Proteomics Facility for the identification of MK2-ubiquitinated residues. We acknowledge the excellent technical assistance of the Universitat de Barcelona Fluorescence-Activated Cell Sorting Flow Cytometry facility. This work was supported by European Research Council Grant 294665, Spanish Ministerio de Ciencia e Innovación (MICINN) Grants SAF2016-81043-R and PID2019-109521RB-I00, and Agència de Gestió D'Ajuts Universitaris I de Recerca (AGAUR) Grant 2017 SRG-557. IRB Barcelona is the recipient of institutional funding from MICINN through the Centers of Excellence Severo Ochoa award and from the Centres de Recerca de Catalunya (CERCA) Program of the Catalan Government.

1. N. Trempolec, N. Dave-Coll, A. R. Nebreda, SnapShot: p38 MAPK substrates. *Cell* **152**, 924–924.e1 (2013).
2. J. Han, J. Wu, J. Silke, An overview of mammalian p38 mitogen-activated protein kinases, central regulators of cell stress and receptor signaling. *F1000Res.* **9**, 653 (2020).
3. I. A. Manke *et al*., MAPKAP kinase-2 is a cell cycle checkpoint kinase that regulates the G2/M transition and S phase progression in response to UV irradiation. *Mol. Cell* **17**, 37–48 (2005).
4. M. E. Borisova *et al*., p38-MK2 signaling axis regulates RNA metabolism after UV-light-induced DNA damage. *Nat. Commun.* **9**, 1017 (2018).
5. N. Trempolec *et al*., Induction of oxidative metabolism by the p38α/MK2 pathway. *Sci. Rep.* **7**, 11367 (2017).
6. F. Köpper *et al*., Damage-induced DNA replication stalling relies on MAPK-activated protein kinase 2 activity. *Proc. Natl. Acad. Sci. U.S.A.* **110**, 16856–16861 (2013).
7. E. Rodríguez-Carballo, B. Gámez, F. Ventura, p38 MAPK signaling in osteoblast differentiation. *Front. Cell Dev. Biol.* **4**, 40–40 (2016).
8. F. B. Engel *et al*., p38 MAP kinase inhibition enables proliferation of adult mammalian cardiomyocytes. *Genes Dev.* **19**, 1175–1187 (2005).
9. B. Canovas, A. R. Nebreda, Diversity and versatility of p38 kinase signalling in health and disease. *Nat. Rev. Mol. Cell. Biol.* **22**, 346–366 (2021).
10. J. E. Purvis, G. Lahav, Encoding and decoding cellular information through signaling dynamics. *Cell* **152**, 945–956 (2013).
11. J. R. Perkins, I. Diboun, B. H. Dessailly, J. G. Lees, C. Orengo, Transient protein-protein interactions: Structural, functional, and network properties. *Structure* **18**, 1233–1243 (2010).
12. J. Westermarck, J. Ivaska, G. L. Corthals, Identification of protein interactions involved in cellular signaling. *Mol. Cell. Proteomics* **12**, 1752–1763 (2013).
13. K. Stojanovski *et al*., Interaction dynamics determine signaling and output pathway responses. *Cell Rep.* **19**, 136–149 (2017).
14. A. White, C. A. Pargellis, J. M. Studts, B. G. Werneburg, B. T. Farmer II, Molecular basis of MAPK-activated protein kinase 2:p38 assembly. *Proc. Natl. Acad. Sci. U.S.A.* **104**, 6353–6358 (2007).
15. G. Tan, J. Niu, Y. Shi, H. Ouyang, Z. H. Wu, NF-κB-dependent microRNA-125b up-regulation promotes cell survival by targeting p38α upon ultraviolet radiation. *J. Biol. Chem.* **287**, 33036–33047 (2012).
16. A. Kuzmanic *et al*., Changes in the free-energy landscape of p38α MAP kinase through its canonical activation and binding events as studied by enhanced molecular dynamics simulations. *eLife* **6**, e22175 (2017).
17. P. Sok *et al*., MAP kinase-mediated activation of RSK1 and MK2 substrate kinases. *Structure* **28**, 1101–1113.e5 (2020).
18. C. Ambrosino *et al*., Negative feedback regulation of MKK6 mRNA stability by p38alpha mitogen-activated protein kinase. *Mol. Cell. Biol.* **23**, 370–381 (2003).
19. J. H. Hu *et al*., Feedback control of MKP-1 expression by p38. *Cell. Signal.* **19**, 393–400 (2007).
20. P. C. Cheung, D. G. Campbell, A. R. Nebreda, P. Cohen, Feedback control of the protein kinase TAK1 by SAPK2a/p38alpha. *EMBO J.* **22**, 5793–5805 (2003).
21. C. J. Caunt, S. M. Keyse, Dual-specificity MAP kinase phosphatases (MKPs): Shaping the outcome of MAP kinase signalling. *FEBS J.* **280**, 489–504 (2013).
22. A. Cuadrado, A. R. Nebreda, Mechanisms and functions of p38 MAPK signalling. *Biochem. J.* **429**, 403–417 (2010).
23. W. Fan *et al*., Hsp70 interacts with mitogen-activated protein kinase (MAPK)-activated protein kinase 2 to regulate p38MAPK stability and myoblast differentiation during skeletal muscle regeneration. *Mol. Cell. Biol.* **38**, e00211–e00218 (2018).
24. A. Cuenda, S. Rousseau, p38 MAP-kinases pathway regulation, function and role in human diseases. *Biochim. Biophys. Acta* **1773**, 1358–1375 (2007).
25. J. Gupta, A. R. Nebreda, Roles of p38α mitogen-activated protein kinase in mouse models of inflammatory diseases and cancer. *FEBS J.* **282**, 1841–1857 (2015).

26. P. Trulley *et al*., Alternative translation initiation generates a functionally distinct isoform of the stress-activated protein kinase MK2. *Cell Rep.* **27**, 2859–2870.e6 (2019).
27. M. B. Menon, M. Gaestel, MK2-TNF-signaling comes full circle. *Trends Biochem. Sci.* **43**, 170–179 (2018).
28. K. Soukup *et al*., Loss of MAPK-activated protein kinase 2 enables potent dendritic cell-driven anti-tumour T cell response. *Sci. Rep.* **7**, 11746 (2017).
29. L. Latonen, Y. Taya, M. Laiho, UV-radiation induces dose-dependent regulation of p53 response and modulates p53-HDM2 interaction in human fibroblasts. *Oncogene* **20**, 6784–6793 (2001).
30. S. Regot, J. J. Hughey, B. T. Bajar, S. Carrasco, M. W. Covert, High-sensitivity measurements of multiple kinase activities in live single cells. *Cell* **157**, 1724–1734 (2014).
31. S. M. Lukas *et al*., Catalysis and function of the p38 alpha.MK2a signaling complex. *Biochemistry* **43**, 9950–9960 (2004).
32. S. López-Avilés *et al*., Activation of Srk1 by the mitogen-activated protein kinase Sty1/Spc1 precedes its dissociation from the kinase and signals its degradation. *Mol. Biol. Cell* **19**, 1670–1679 (2008).
33. T. Moriguchi *et al*., Purification and identification of a major activator for p38 from osmotically shocked cells. Activation of mitogen-activated protein kinase kinase 6 by osmotic shock, tumor necrosis factor-alpha, and H_2O_2. *J. Biol. Chem.* **271**, 26981–26988 (1996).
34. T. Sudo, K. Kawai, H. Matsuzaki, H. Osada, p38 mitogen-activated protein kinase plays a key role in regulating MAPKAPK2 expression. *Biochem. Biophys. Res. Commun.* **337**, 415–421 (2005).
35. P. R. Mittelstadt, H. Yamaguchi, E. Appella, J. D. Ashwell, T cell receptor-mediated activation of p38alpha by mono-phosphorylation of the activation loop results in altered substrate specificity. *J. Biol. Chem.* **284**, 15469–15474 (2009).
36. I. Dikic, Proteasomal and autophagic degradation systems. *Annu. Rev. Biochem.* **86**, 193–224 (2017).
37. I. Livneh, V. Cohen-Kaplan, C. Cohen-Rosenzweig, N. Avni, A. Ciechanover, The life cycle of the 26S proteasome: From birth, through regulation and function, and onto its death. *Cell Res.* **26**, 869–885 (2016).
38. G. Ben-Nissan, M. Sharon, Regulating the 20S proteasome ubiquitin-independent degradation pathway. *Biomolecules* **4**, 862–884 (2014).
39. A. M. Pickering, K. J. Davies, Degradation of damaged proteins: The main function of the 20S proteasome. *Prog. Mol. Biol. Transl. Sci.* **109**, 227–248 (2012).
40. X. Wang *et al*., The 19S Deubiquitinase inhibitor b-AP15 is enriched in cells and elicits rapid commitment to cell death. *Mol. Pharmacol.* **85**, 932–945 (2014).
41. Y. Song *et al*., Blockade of deubiquitylating enzyme Rpn11 triggers apoptosis in multiple myeloma cells and overcomes bortezomib resistance. *Oncogene* **36**, 5631–5638 (2017).
42. K. I. Nakayama, K. Nakayama, Ubiquitin ligases: Cell-cycle control and cancer. *Nat. Rev. Cancer* **6**, 369–381 (2006).
43. C. E. Berndsen, C. Wolberger, New insights into ubiquitin E3 ligase mechanism. *Nat. Struct. Mol. Biol.* **21**, 301–307 (2014).
44. Y. Li *et al*., An integrated bioinformatics platform for investigating the human E3 ubiquitin ligase-substrate interaction network. *Nat. Commun.* **8**, 347 (2017).
45. Y. Haupt, R. Maya, A. Kazaz, M. Oren, Mdm2 promotes the rapid degradation of p53. *Nature* **387**, 296–299 (1997).
46. M. H. Kubbutat, S. N. Jones, K. H. Vousden, Regulation of p53 stability by Mdm2. *Nature* **387**, 299–303 (1997).
47. M. Gaestel, What goes up must come down: Molecular basis of MAPKAP kinase 2/3-dependent regulation of the inflammatory response and its inhibition. *Biol. Chem.* **394**, 1301–1315 (2013).
48. B. Liu *et al*., A functional copy-number variation in MAPKAPK2 predicts risk and prognosis of lung cancer. *Am. J. Hum. Genet.* **91**, 384–390 (2012).
49. M. Guo *et al*., Targeting MK2 is a novel approach to interfere in multiple myeloma. *Front. Oncol.* **9**, 722 (2019).
50. N. Ronkina *et al*., The mitogen-activated protein kinase (MAPK)-activated protein kinases MK2 and MK3 cooperate in stimulation of tumor necrosis factor biosynthesis and stabilization of p38 MAPK. *Mol. Cell. Biol.* **27**, 170–181 (2007).
51. K. Kirsch *et al*., Co-regulation of the transcription controlling ATF2 phosphoswitch by JNK and p38. *Nat. Commun.* **11**, 5769 (2020).
52. M. F. Lavin, N. Gueven, The complexity of p53 stabilization and activation. *Cell Death Differ.* **13**, 941–950 (2006).
53. H. F. Horn, K. H. Vousden, Coping with stress: Multiple ways to activate p53. *Oncogene* **26**, 1306–1316 (2007).
54. T. Tomida, M. Takekawa, H. Saito, Oscillation of p38 activity controls efficient pro-inflammatory gene expression. *Nat. Commun.* **6**, 8350 (2015).
55. H. Ju *et al*., Sustained activation of p38 mitogen-activated protein kinase contributes to the vascular response to injury. *J. Pharmacol. Exp. Ther.* **301**, 15–20 (2002).
56. M. Warny *et al*., p38 MAP kinase activation by Clostridium difficile toxin A mediates monocyte necrosis, IL-8 production, and enteritis. *J. Clin. Invest.* **105**, 1147–1156 (2000).
57. I. Darlyuk-Saadon *et al*., Expression of a constitutively active p38α mutant in mice causes early death, anemia, and accumulation of immunosuppressive cells. *FEBS J.* 10.1111/febs.15697. (2021).
58. U. M. Moll, O. Petrenko, The MDM2-p53 interaction. *Mol. Cancer Res.* **1**, 1001–1008 (2003).
59. A. Bugai *et al*., P-TEFb activation by RBM7 shapes a pro-survival transcriptional response to genotoxic stress. *Mol. Cell* **74**, 254–267.e10 (2019).
60. D. V. Bulavin *et al*., Phosphorylation of human p53 by p38 kinase coordinates N-terminal phosphorylation and apoptosis in response to UV radiation. *EMBO J.* **18**, 6845–6854 (1999).
61. X. Gong, X. Ming, P. Deng, Y. Jiang, Mechanisms regulating the nuclear translocation of p38 MAP kinase. *J. Cell. Biochem.* **110**, 1420–1429 (2010).
62. A. Porras *et al*., P38 alpha mitogen-activated protein kinase sensitizes cells to apoptosis induced by different stimuli. *Mol. Biol. Cell* **15**, 922–933 (2004).
63. Y. W. Kong *et al*., Enhancing chemotherapy response through augmented synthetic lethality by co-targeting nucleotide excision repair and cell-cycle checkpoints. *Nat. Commun.* **11**, 4124 (2020).
64. H. C. Reinhardt, A. S. Aslanian, J. A. Lees, M. B. Yaffe, p53-deficient cells rely on ATM- and ATR-mediated checkpoint signaling through the p38MAPK/MK2 pathway for survival after DNA damage. *Cancer Cell* **11**, 175–189 (2007).
65. H. Miura, Y. Kondo, M. Matsuda, K. Aoki, Cell-to-cell heterogeneity in p38-mediated cross-inhibition of JNK causes stochastic cell death. *Cell Rep.* **24**, 2658–2668 (2018).
66. T. Thuraisingam *et al*., MAPKAPK-2 signaling is critical for cutaneous wound healing. *J. Invest. Dermatol.* **130**, 278–286 (2010).